Epidemic Model with Isolation in Multilayer Networks

L. G. Alvarez Zuzek,[1,*] H. E. Stanley,[2] and L. A. Braunstein[1,2]

[1]*Departamento de Física, Facultad de Ciencias Exactas y Naturales, Universidad Nacional de Mar del Plata, and Instituto de Investigaciones Físicas de Mar del Plata (IFIMAR-CONICET), Deán Funes 3350, 7600 Mar del Plata, Argentina*

[2]*Center for Polymer Studies, Boston University, Boston, Massachusetts 02215, USA.*

Abstract

The Susceptible-Infected-Recovered (SIR) model has successfully mimicked the propagation of such airborne diseases as influenza A (H1N1). Although the SIR model has recently been studied in a multilayer networks configuration, in almost all the research the isolation of infected individuals is disregarded. Hence we focus our study in an epidemic model in a two-layer network, and we use an isolation parameter to measure the effect of isolating infected individuals from both layers during an isolation period. We call this process the Susceptible-Infected-Isolated-Recovered (SI_IR) model. The isolation reduces the transmission of the disease because the time in which infection can spread is reduced. In this scenario we find that the epidemic threshold increases with the isolation period and the isolation parameter. When the isolation period is maximum there is a threshold for the isolation parameter above which the disease never becomes an epidemic. We also find that epidemic models, like SIR overestimate the theoretical risk of infection. Finally, our model may provide a foundation for future research to study the temporal evolution of the disease calibrating our model with real data.

*Electronic address: lgalvere@mdp.edu.ar

INTRODUCTION

Most real-world systems can be modeled as complex networks in which nodes represent such entities as individuals, companies, or computers and links represent the interactions between them. In recent decades researchers have focused on the topology of these networks [1]. Most recently this focus has been on the processes that spread across networks, e.g., synchronization [2, 3], diffusion [4], percolation [5–8], or the propagation of epidemics [9–17]. Epidemic spreading models have been particularly successfully in explaining the propagation of diseases and thereby have allowed the development of mitigation strategies for decreasing the impact of diseases on healthy populations.

A commonly-used model for reproducing disease spreading dynamics in networks is the susceptible-infected-recovered (SIR) model [18, 19]. It has been used to model such diseases as seasonal influenza, such as the SARS [20]. This model groups the population of individuals to be studied into three compartments according to their state: the susceptible (S), the infected (I), and the recovered (R). When a susceptible node comes in contact with an infected node it becomes infected with a probability β and after a period of time t_r it recovers and becomes immune. When the parameters β and t_r are made constant, the effective probability of infection is given by the transmissibility $T = 1 - (1 - \beta)^{t_r}$ [5, 21].

As infected individuals cannot be reinfected, the SIR model has a tree-like structure with branches of infection that develop and expand. Because in its final state this process can be mapped into link percolation [7, 22], we use a generating function to describe it. In this framework, the most important magnitude is the probability f that a branch of infection will expand throughout the network, [1, 22]. When a branch of infection reaches a node with k connections across one of its links, it can only expand through its $k - 1$ remaining connections. It can be shown that f verifies the self-consistent equation $f = 1 - G_1(1 - Tf)$, where $G_1(x) = \sum_{k=k_{min}}^{k_{max}} kP(k)/\langle k \rangle x^{k-1}$ is the generating function of the underlying branching process [7]. Note that $G_1(x)$ here represents the probability that the branches of infection will not expand throughout the network. At the final state of this process, the branches of infection contribute to a spanning cluster of recovered, previously infected individuals. Thus the probability of selecting a random node that belongs to the spanning cluster is given by $R = 1 - G_0(1 - Tf)$, where $G_0 = \sum_{k=k_{min}}^{k_{max}} P(k)x^k$ is the

generating function of the degree distribution. When $T \leq T_c$ there is an epidemic-free phase with only small outbreaks, which correspond to finite cluster in link percolation theory. But, when $T > T_c$ an epidemic phase develops. In isolated networks the epidemic threshold is given by $T_c = 1/(\kappa - 1)$, where κ is the branching factor that is a measure of the heterogeneity of the network. The branching factor is defined as $\kappa \equiv \langle k^2 \rangle / \langle k \rangle$, where $\langle k^2 \rangle$ and $\langle k \rangle$ are the second and first moment of the degree distribution, respectively.

Because real-world networks are not isolated, in recent years scientific researchers have focused their attention on multilayer networks, i.e., on "networks of networks" [23–36]. In multilayer networks, individuals can be actors on different layers with different contacts in each layer. This is not necessarily the case in interacting networks. Dickinson *et al.* [37] studied numerically the SIR model in two networks that interact through inter-layer connections given by a degree distribution. There is a probability that these inter-layer connections will allow infection to spread between nodes in different layers. They found that, depending on the average degree of the inter-layer connections, one layer can be in an epidemic-free phase and the other in an epidemic phase. Yagan *et al.* [38] studied the SIR model in two multilayer networks in which all the individuals act in both layers. In their model the transmissibility is different in each network because one represents the virtual contact network and the other the real contact network. They found that the multilayer structure and the presence of the actors in both layers make the propagation process more efficient and thus increase the theoretical risk of infection above that found in isolated networks. This can have catastrophic consequences for the healthy population. Sanz *et al.* [16] studied the spreading dynamics and the temporal evolution of two concurrent diseases that interact with each other in a two-layer network system, for different epidemic models. In particular, they found that for the SIR in the final state this interaction can determinate the values of the epidemic threshold of one of the diseases whose dynamic has been modified by the presence of the other disease. Buono *et al.* [39] studied the SIR model, with β and t_r constant, in a system composed of two overlapping layers in which only a fraction q of individuals can act in both layers. In their model, the two layers represent contact networks in which only the overlapping nodes enable the propagation, and thus the transmissibility T is the same in both layers. They found that decreasing the overlap decreases the risk of an epidemic compared to when there is a full overlap ($q = 1$).

All of the above research assumes that individuals, independent of their state, will continue acting in many layers. In a real-world scenario, however, an infected individual may be isolated for a period of time and thus may not be able to act in other layers, e.g., for a period of time they may not be able to go to work or visit friends and may have to stay at home or be hospitalized. Thus the propagation of the disease is reduced. This scenario is more realistic than the one in which an actor continues to participate in all layers irrespective of their state [38, 39]. As we will demonstrate, compared to the theoretical risk measurement produced by multilayer network SIR models, our approach more accurately measures the decrease in the theoretical risk of epidemic propagation.

RESULTS

Model and Simulation Results

We consider the case of a two-layer network, A and B, of equal size N, where one layer represents an individual's work environment and the other their social environment. The degree distribution in each layer is given by $P_i(k)$, with $i = A, B$ and $k_{\min} \leq k \leq k_{\max}$, where $k_{\min}$ and $k_{\max}$ are the minimum and the maximum degree allowed a node.

At the initial stage all individuals in both layers are susceptible nodes. We randomly infect an individual in layer A. At the beginning of the propagation process, each infected individual is isolated from both layers with a probability w for a period of time t_w. For simplicity, in our epidemic model we assume that every infected individual is isolated from both layers with the same probability w during a period of time t_w. The probability that an infected individual is not isolated from both layers is thus $1 - w$. At each time step, a non-isolated infected individual spreads the disease with a probability β during a time interval t_r after which he recover. When an individual j after t_w time steps is no longer isolated he reverts to two possibles states. When $t_w < t_r$, j will be infected in both layers for only $t_r - t_w$ time steps and the infection transmissibility of j is reduced from $1 - (1 - \beta)^{t_r}$ to $1 - (1 - \beta)^{t_r - t_w}$, but when $t_w \geq t_r$, j recovers and no longer spreads the disease. At the final stage of the propagation all of the individuals are either susceptible or recovered. The overall transmissibility $T^* \equiv T^*_{\beta, t_r, t_w, w}$ is the probability that an infected individual will transmit the disease to their neighbors. This probability takes into account

that the infected is either isolated or non-isolated in both layers for a period of time and is given by

$$T^* \;=\; 1 - \Big[(1-w)\,(1-\beta)^{t_r} + w\,(1-\beta)^{t_r - t_w}\Big]. \tag{1}$$

Here the second and third term takes into account non-isolated and isolated individuals and represents the probabilities that this infected individual does not transmit the disease during t_r and $t_r - t_w$ time steps respectively.

Mapping this process onto link percolation in two layers, we can write two self-consistent coupled equations, f_i, $i = A, B$, for the probability that in a randomly chosen edge traversed by the disease there will be a node that facilitates an infinite branch of infection throughout the two-layer network, i.e.,

$$\begin{aligned} f_A &= [1 - G_1^A\,(1 - T^* f_A)\,G_0^B(1 - T^* f_B)] \\ f_B &= [1 - G_1^B(1 - T^* f_B)\,G_0^A(1 - T^* f_A)], \end{aligned} \tag{2}$$

where $G_0^{A/B}$ and $G_1^{A/B}$ are the generating function defined in the Introduction for layer A and B. Here $G_1^{A/B}$ takes into account the probability that a branch of infection reaches a node in layer A/B of connectivity k across one of its links and cannot expand through its remaining $k-1$ connection. Then $G_0^{A/B}$ represents the probability that the branch of infection propagates from one layer into the other, reaches a node, but cannot expand through all of its connections. Figure (1) shows a schematic of the contributions to Eqs. (2).

Using the nontrivial roots of Eq. (2) we compute the order parameter of the phase transition, which is the fraction of recovered nodes R, where R is given by

$$R = 1 - G_0^A\,(1 - T^* f_A)\,G_0^B(1 - T^* f_B). \tag{3}$$

Note that in the final state of the process the fraction of recovered nodes in layers A and B are equal because all nodes are present in both layers. From Eqs. (1) and (2) we see that if we use the overall transmissibility T^* as the control parameter we lose information about w, the isolation parameter, and t_w, the characteristic time of the isolation. In our model we thus use $\beta \equiv \beta_{T^*}$ as the control parameter, where β is obtained by inverting Eq. (1) with fixed t_r [40].

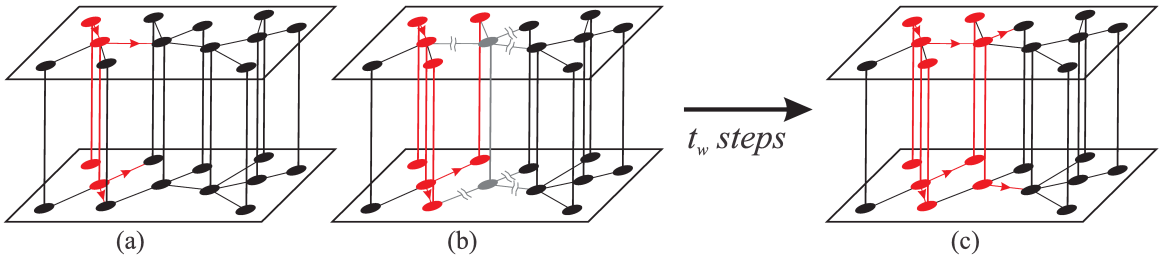

FIG. 1: Schematic of a multilayer network consisting of two layers, each of size $N = 12$. The black nodes represent the susceptible individuals and the red nodes the infected individuals. In this case, we consider $t_w < t_r$. (a) The red arrows indicate the direction of the branches of infection. All the branches spreads through A and B because the infected nodes are not isolated and thus interact in both layers. (b) The gray node, represents an individual who is isolated from both layers for a period of time t_w. (c) After t_w time steps the gray node in (b) is no longer isolated, and can infect its neighbors in A and B, if they were not reach by another branch of infection, during $t_r - t_w$ time steps (Color on line).

Figure 2 shows a plot of the order parameter R as a function of β for different values of w, with $t_r = 6$ and $t_w = 4$ obtained from Eq. (3) and from the simulations. For (a) we consider two Erdős-Rényi (ER) networks [41], which have a Poisson degree distribution and an average degree $\langle k_A \rangle = \langle k_B \rangle = 2$, and for (b) we consider two scale free networks with an exponential cutoff $c = 20$ [7], where $P_i(k_i) \sim k_i^{-\lambda_i} e^{-k_i/c}$, with $\lambda_A = 2.5$ and $\lambda_B = 3.5$. We use this type of SF network because it represents many structures found in real-world systems [42, 43].

In the simulations we construct two networks of equal size using the Molloy-Reed algorithm [44], and we randomly overlap one-to-one the nodes in network A with the nodes of networks B. We assume that an epidemic occurs at each realization if the number of recovered individuals is greater than 200 for a system size of $N = 10^5$ [45]. Realizations with fewer than 200 recovered individuals are considered outbreaks and are disregarded.

Figure 2 shows an excellent agreement between the theoretical equations (see Eq. 3) and the simulation results. The plot shows that the critical threshold β_c increases with w, which indicates that the theoretical risk for an epidemic decreases with the isolation

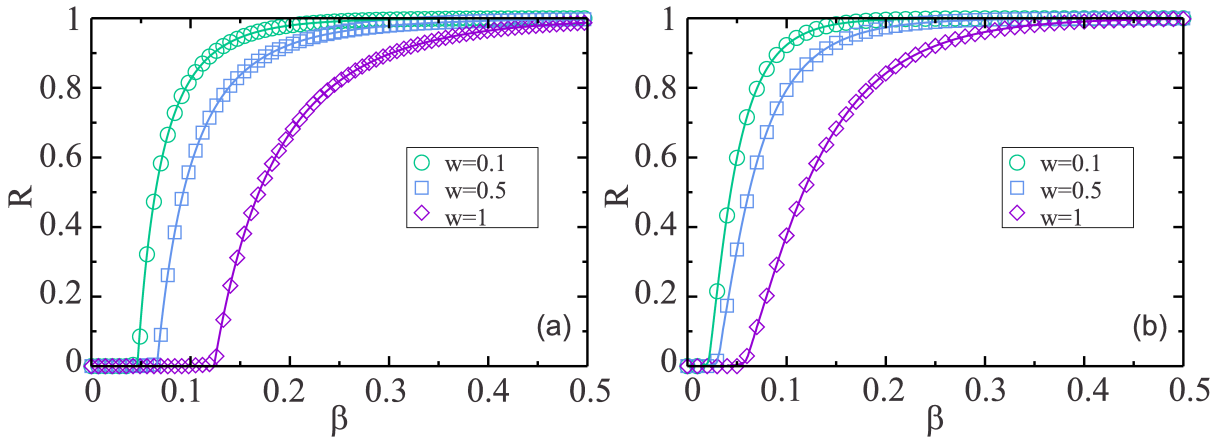

FIG. 2: Simulations and theoretical results of the total fraction of recovered nodes R, in the final state of the process, as a function of β, with $t_r = 6$ and $t_w = 4$, for different values of w. The full lines corresponds to the theoretical evaluation of Eq. 3 and the symbols corresponds to the simulations results, for $w = 0.1$ (◯) in green, $w = 0.5$ (□) in blue and $w = 1$ (◇) in violet. The multilayer network is consisted by two layers, each of size $N = 10^5$. For (a) two ER layers with $\langle k_A \rangle = \langle k_B \rangle = 2$, $k_{\min} = 1$ and $k_{\max} = 40$ and (b) two scale free networks with $\lambda_A = 2.5$, $\lambda_B = 3.5$ and exponential cutoff $c = 20$ with $k_{\min} = 2$ and $k_{\max} = 250$ (Color online).

parameter w. Note that above the threshold but near it R decreases as the isolation w increases, indicating that isolation for even a brief period of time reduces the propagation of the disease. The critical threshold β_c is at the intersection of the two Eqs. (2) where all branches of infection stop spreading, i.e., $f_A = f_B = 0$. This is equivalent to finding the solution of the system $det(J - I) = 0$, where J is the Jacobian of the coupled equation with $J_{i,k}|_{f_i=f_k=0} = \partial f_i/\partial f_k|_{f_i=f_k=0}$ and I is the identity, and

$$T_c^{*\,2}\,[(\kappa_A - 1)(\kappa_B - 1) - \langle k_A \rangle \langle k_B \rangle] - T_c^*[(\kappa_A - 1) + (\kappa_B - 1)] + 1 \;=\; 0, \qquad (4)$$

where κ_A and κ_B are the branching factor of layers A and B, and $\langle k_A \rangle$ and $\langle k_B \rangle$ are their average degree. Using numerical evaluations of the roots of Eq. (4) we find the physical and stable solution for the critical threshold β_c, which corresponds to the smaller root of Eq. (4) [46]. Figure 3 shows a plot of the phase diagram in the plane $\beta - w$ for (a) two ER multilayer networks [41] with average degree $\langle k_A \rangle = \langle k_B \rangle = 2$ and (b) two power law networks with an exponential cutoff $c = 20$ [7], with $\lambda_A = 2.5$ and $\lambda_B = 3.5$. In both Fig. 4 and Fig. 3 we use $t_r = 6$ and values $t_w = 0$, 1, 2, 3, 4, 5, and 6, from bottom to

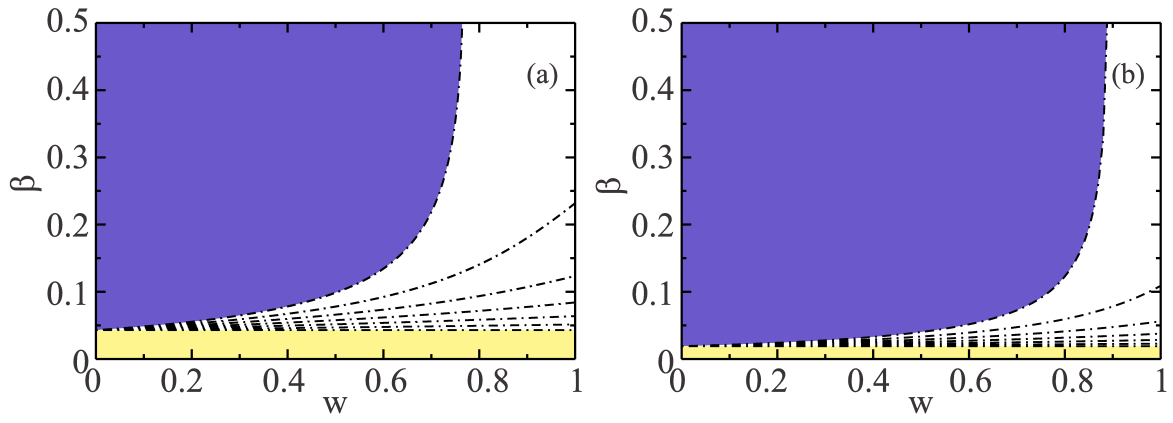

FIG. 3: Phase diagram in the plane $\beta - w$. In both plots, we consider $t_r = 6$ and $t_w = 0, 1, 2, 3, 4, 5, 6$ from bottom to top for (a) two ER networks with $\langle k_A \rangle = \langle k_B \rangle = 2$ with $k_{\min} = 1$ and $k_{\max} = 40$. (b) two power law networks with $\lambda_A = 2.5$ and $\lambda_B = 3.5$ with $k_{\min} = 2$ and $k_{\max} = 250$ and exponential cutoff $c = 20$. The region above each line corresponds to the Epidemic phase and the region below correspond to the Epidemic-free phase. In the limit of $w \to 0$ and for $t_w = 0$ we recover the SIR in multiplex networks with (a) $\beta_c \approx 0.043$ and (b) $\beta_c \approx 0.019$. For the case $t_r = t_w$, there is a threshold for w with (a) $w_c = 0.76$ and (b) $w_c = 0.88$, above which there is only an Epidemic-free phase.

top.

The regions below the curves shown in Fig. 3 correspond to the epidemic-free phase. Note that for different values of t_w those regions widen as w increases. Note also that when $t_r = t_w$ there is a threshold w_c above which, irrespective of the theoretical risk (β_c), the disease never becomes an epidemic. For $t_w = 0$ and $w = 0$ we recover the SIR process in a two-layer network system that corresponds to $\beta_c \approx 0.043$ with $k_{\min} = 1$ and $k_{\max} = 40$ [47] in Fig. 3(a) and $\beta_c \approx 0.019$ with $k_{\min} = 2$ and $k_{\max} = 250$ in Fig. 3(b). Although in the limit $c \to \infty$, $\beta_c \to 0$, and most real-world networks are not that heterogeneous and exhibit low values of c [9, 42].

As expected and confirmed by our model, the best way to stop the propagation of a disease before it becomes an epidemic is to isolate the infected individuals in both layers until they recover, which corresponds to $t_w = t_r$ and $w > 0$. Because this is strongly dependent upon the resources of the location from which the disease begins to spread and

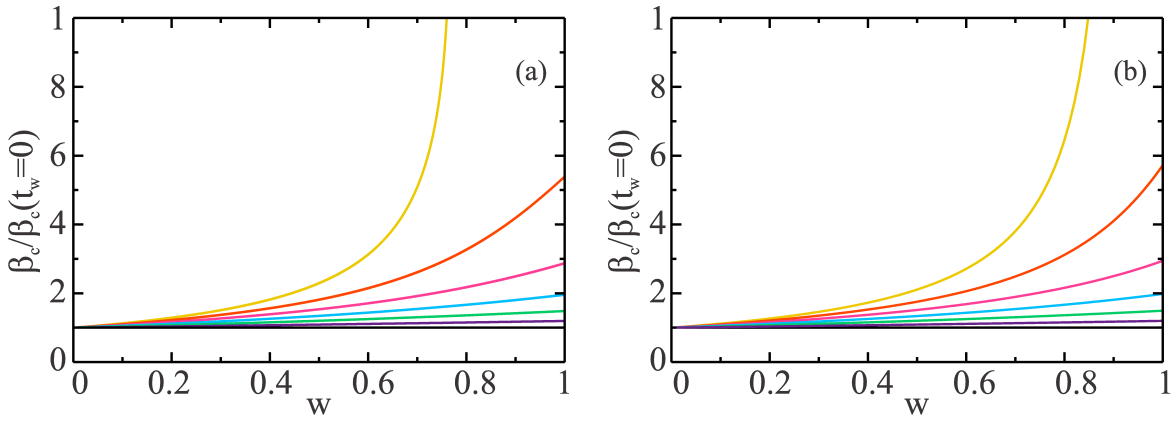

FIG. 4: Ratio of $\beta_c(t_w)$ to $\beta_c(0)$ as a function of w. For $t_w = 1, 2, 3, 4, 5, 6$ from bottom to top for (a) two ER networks with $\langle k_A \rangle = \langle k_A \rangle = 2$ with $k_{\min} = 1$ and $k_{\max} = 40$ and (b) two power law networks with $\lambda_A = 2.5$ and $\lambda_B = 3.5$ with $k_{\min} = 2$ and $k_{\max} = 250$, with exponential cutoff $c = 20$. In both Figures, the limit $w \to 0$ correspond to a SIR process, and as w increases the overestimation increases.

on each infected patient's knowledge of the consequences of being in contact with healthy individuals, the isolation procedure can be difficult to implement.

We also study a case in which there is isolation in one layer (for a detailed description see Supplementary Information). We find that, for all values of β, there is no critical value of w above which the phase is epidemic-free, *i.e.* the disease never becomes an epidemic.

The phase diagram indicates that when the SIR model is applied to multilayer networks, which corresponds to the case $t_w = 0$, it overestimates the theoretical risk β_c of an epidemic. This theoretical overestimation can strongly affect the spreading dynamics. Figure 4(a) plots the ratio $\beta_c/\beta_c(t_w = 0)$ as a function of w for different values of t_w, with $t_w > 0$ for two ER networks. Figure 4(b) shows how much the theoretical risk is overestimated in the SIR model of a two-layer SF networks. Note that in order to estimate the real epidemic risk the model must fit data from where the estimated transmission parameter, β, can be obtained. This is a difficult task when using theoretical networks because the structure of the contact network, where the epidemic propagation takes place, is not known, and in general these problems are solved using meta-population [48, 49] networks or a full-mixing approach [50–52].

In the limit $t_w = 0$ and $w \to 0$ we revert to the SIR model in multilayer networks [39]. As w increases and when $t_w \neq 0$ there is always an overestimation of the theoretical risk. Note that when $t_w = t_r$ the plot shows that when the percentage of infected individuals who are hospitalized or isolated in their homes is approximately 40, for two ER, and 50 percent, for two SF, the SIR model indicates double the actual theoretical risk of infection. The declaration of an epidemic by a government health service is a non-trivial decision, and can cause panic and negatively effect the economy of the region. Thus any epidemic model of airborne diseases that spread in multilayer networks, if the projected scenario is to be realistic and in agreement with the available real data, must take into account that some infected individuals will be isolated for a period of time. In particular, in such diseases as the recent outbreak of Ebola in Western Africa, in which the hospitalization of patients is a significant factor strongly affecting the propagation of the outbreak, research must take this hospitalization into account [48, 50–52]. Note also that this isolation can also delay the onset of the peak of the epidemic and thus allow health authorities more time to make interventions. This is an important topic for future investigation.

Discussion

In summary, we study a SIR epidemic model in two multilayer networks in which infected individuals are isolated from both layers with probability w during a period of time t_w. Using a generating function framework, we compute the total fraction of recovered nodes in the steady state as a function of the probability of infection β and find a perfect agreement between the theoretical and the simulation results. We derive an expression for the epidemic threshold and we find that β_c increases as w and t_w increase. For $t_w = t_r$ we find a critical threshold w_c above which any disease can be stopped before it becomes an epidemic and which cannot be found when isolating only in one layer. From our results we also note that as the isolation parameter and the period of isolation increases the overestimation increases. Our model enables us to conclude that the SIR model of multilayer networks overestimates the theoretical risk of infection. This finding is highly relevant to the work of researchers developing epidemic models. Our model can also provide a foundation for estimating the real value of β through a data driven model that could be used by health authorities when implementing policies for stopping a disease

before it becomes an epidemic.

Acknowledgments

We thank the NSF (grants CMMI 1125290 and CHE-1213217) and the Keck Foundation for financial support. LGAZ and LAB wish to thank to UNMdP and FONCyT (Pict 0429/2013) for financial support.

Additional information The authors declare no competing financial interests. Supplementary information is available in the online version of the paper. Reprints and permissions information is available online at www.nature.com/reprints. Correspondence and requests for materials should be addressed to L.G.A.Z.

---

[1] Albert R. & Barabási A. L. Statistical mechanics of complex networks. *Rev. Mod. Phys.* **74**, 47-97 (2002).

[2] La Rocca C. E., Braunstein L. A. & Macri P. A. Conservative model for synchronization problems in complex netwrks. *Phys. Rev. E.* **80**, 026111 (2009).

[3] Pastore y Piontti A., Macri P. A. & Braunstein L. A. Discrete surface growth process as a synchronization mechanism for scale free complex networks. *Phys. Rev. E.* **76**, 046117 (2007).

[4] Gallos L. K. & Argyrakis P. Absence of kinetic effects in reaction-diffusion processes in scale-free networks. *Phys. Rev. Lett.* **92**, 138301 (2004).

[5] Callaway D. S., Newman M. E. J., Strogatz S. H. & Watts D. J. Network Robustness and Fragility: Percolation on Random Graphs. *Phys. Rev. Lett.* **85**, 5468 (2000).

[6] Cohen R., Havlin S. & Ben-Avraham D. Efficient Immunization Strategies for Computer Networks and Populations. *Phys. Rev. Lett.* **91**, 247901 (2003).

[7] Newman M. E. J., Strogatz S. H. & Watts D. J. Random graphs with arbitrary degree distributions and their applications. *Phys. Rev. E* **64**, 026118 (2001).

[8] Valdez L. D., Buono C., Macri P. A. & Braunstein L. A. Effect of degree correlations above the first shell on the percolation transition. *Europhysics lett.* **96**, 38001 (2011).

[9] Newman M. E. J. Spread of epidemic disease on networks. *Phys. Rev. E.* **66**, 016128 (2002).

[10] Pastor-Satorras R. & Vespignani A. Epidemic Spreading in Scale-Free Networks. *Phys. Rev. Lett.* **86**, 3200 (2001).

[11] Buono C., Vazquez F., Macri P. A. & Braunstein L. A. Slow epidemic extinction in populations with heterogeneous infection rates. *Phys. Rev. E.* **88**, 022813 (2013).

[12] Pastor-Satorras R. & Vespignani A. Epidemic dynamics and endemic states in complex networks. *Phys. Rev. E.* **63**, 066117 (2001).

[13] Granell C., Gómez S. & Arenas A. Dynamical Interplay between Awareness and Epidemic Spreading in Multiplex Networks. *Phys. Rev. Lett.* **111**, 128701 (2013).

[14] Cozzo E., Baños R. A., Meloni S. & Moreno Y. Contact-based Social Contagion in Multiplex Networks. *Phys. Rev. E.* **88**, 050801(R) (2013).

[15] Marceau V., Noël P. A., Hébert-Dufresne L., Allard A. & Dubé L. J. Modeling the dynamical interaction between epidemics on overlay networks. *Phys. Rev. E.* **84**, 026105 (2011).

[16] Sanz J., Xia C., Meloni S. & Moreno Y. Dynamics of Interacting Diseases. *Phys. Rev. X.* **4**, 041005 (2014).

[17] Sahneh F. D. & Scoglio C. Competitive Epidemic Spreading Over Arbitrary Multilayer Networks. *Phys. Rev. E.* **89**, 062817 (2014).

[18] Anderson, R. M., & May, R. M. Infectious diseases of humans. *Oxford university press* **1**.(1991)

[19] Bailey, N. T. The mathematical theory of infectious diseases and its applications. Griffin, London. (1975).

[20] Colizza V., Barrat A., Barthélemy M. & Vespignani A. Predictability and epidemic pathways in global outbreaks of infectious diseases: the SARS case study. *BMC Medicine* **5**, 34 (2007).

[21] Cohen R., Havlin S. & Ben-Avraham D. *Handbook of graphs and networks* (Wiley-VCH, Berlin, 2002), chap. Structural properties of scale free networks.

[22] Braunstein L. A.,*et al.* Optimal path and minimal spanning trees in random weighted networks. *Bifurcation and Chaos* **17**, 2215 (2007).

[23] Buldyrev S. V., Parshani R., Paul G. & Stanley H. E., Havlin S. Catastrophic cascade of failures in interdependent networks. *Nature* **464**, 1025 (2010).

[24] Gao J., Buldyrev S. V., Havlin S. & Stanley H. E. Robustness of a Network of Networks. *Phys. Rev. Lett.* **107**, 195701 (2011).

[25] Gao J., Buldyrev S. V., Stanley H. E & Havlin S. Networks Formed from Interdependent

Networks. *Nature Physics* **8**, 40 (2012).

[26] Dong G., Gao J., Du R., Tian L., Stanley H. E. & Havlin S. Robustness of network of networks under targeted attack. *Phys. Rev. E.* **87**, 052804 (2013).

[27] Valdez L. D., Macri P. A. & Braunstein L. A. Triple point in correlated interdependent networks. *Phys. Rev. E.* **88**, 050803(R) (2013).

[28] Baxter G. J., Dorogovtsev S. N., Goltsev A. V. & Mendes J. F. F. Avalanche Collapse of Interdependent Networks. *Phys. Rev. Lett.* **109**, 248701 (2012).

[29] Brummitt C. D., D'Souza R. M. & Leicht E. A. Suppressing cascades of load in interdependent networks. *Proceedings of the National Academy of Sciences* **109**, 680 (2012).

[30] Brummitt C. D., Lee K.-M. & Goh K.-I. Multiplexity-facilitated cascades in networks. *Phys. Rev. E.* **85**, 045102(R) (2012).

[31] Lee K.-M., Kim Jung Yeol, Cho W. K., Goh K.-I. & Kim I.-M. Correlated multiplexity and connectivity of multiplex random networks. *New Journal of Physics* **14**, 033027 (2012).

[32] Gómez S., Díaz-Guilera A., Gómez-Gardeñes J., Pérez-Vicente C. J., Moreno Y. & Arenas A. Diffusion Dynamics on Multiplex Networks. *Phys. Rev. Lett.* **110**, 028701 (2013).

[33] Kim J. Y. & Goh K.-I. Coevolution and Correlated Multiplexity in Multiplex Networks. *Phys. Rev. Lett.* **111**, 058702 (2013).

[34] Cozzo E., Arenas A. & Moreno Y. Stability of Boolean multilevel networks. *Phys. Rev. E.* **86**, 036115 (2012).

[35] Cardillo A., Gómez-Gardeñes J., Zanin M., Romance M., Papo D., Del Pozo F. & Boccaletti S. Emergence of Network Features from Multiplexity. *Scientific Reports* **3**, 1344 (2013).

[36] Kaluza P., Kölzsch A., Gastner M. T. & Blasius B. The complex network of global cargo ship movements. *Journal of the Royal Society: Interface* **7**, 1093 (2010).

[37] Dickison M., Havlin S. & Stanley H. E. Epidemics on interconnected networks. *Phys. Rev. E.* **85**, 066109 (2012).

[38] Yagan O., Qian D., Zhang J. & Cochran D. Conjoining Speeds up Information Diffusion in Overlaying Social-Physical Networks. *IEEE JSAC Special Issue on Network Science* **31**, 1038 (2013).

[39] Buono C., Alvarez-Zuzek L. G., Macri P. A & Braunstein L. A. Epidemics in partially overlapped multiplex networks. *PLOS ONE* **9**, e92200 (2014).

[40] Note that β and t_r are the intrinsic probability of infection and recovery time of an epidemic

obtained from epidemic data. Thus making t_r constant means that it is the average time of the duration of the disease.

[41] Erdős P. & Rényi A. On Random Graphs. I. *Publications Mathematicae* **6**, 290 (1959).

[42] Amaral L. A. N., Scala A., Barthélemy M. & Stanley H. E. Classes of Small-World Networks. *Proc. Natl. Acad. Sci. USA* **97**, 11149 (2000).

[43] Batagelj, V., & Mrvar, A. Some analyses of Erdos collaboration graph. Social networks, 22(2), 173-186 (2000).

[44] Molloy M & Reed B. A critical point for random graphs with a given degree sequence. *Random Structures and Algorithms* **6:**, 161 180 (1995).

[45] Lagorio C., Migueles M. V., Braunstein L. A. , López E. & Macri P. A. Effects of epidemic threshold definition on disease spread statistics. *Physica A* **388**, 755 (2009).

[46] Alligood K. T., Sauer T. D. & Yorke J. A.*CHAOS: An Introduction to Dynamical Systems.* (*Springer*, 1997).

[47] The value of β_c is obtain from the critical transmisibility $T_c = 1 - (1 - \beta_c)^{t_r} = 1/(\langle k \rangle (1 + (1 - e^{-\langle k \rangle})^{-1}))$.

[48] Gomes M. F. C., Patore y Piontti A., Rossi L., Chao D., Longini I., Halloran M. E. & Vespignani A. Assessing the International Spreading Risk Associated with the 2014 West African Ebola Outbreak. *PLOS Current Outbreaks* doi:10.1371/currents.outbreaks.cd818f63d40e24aef769dda7df9e0da5, (2014).

[49] Balcan D., *et al.*. Multiscale mobility networks and the spatial spreading of Infectious diseases. *Proc Natl Acad Sci 106(51):21484-9.* (2009).

[50] Legrand J., Grais R. F., Boelle P. Y., Valleron A. J. & Flahault A. Understanding the dynamics of Ebola epidemics. *PLOS Current Outbreaks* **135**, 610 (2006).

[51] Rivers C. M., Lofgren E. T., Marathe M., Eubank S. & Lewis B. L. Modeling the Impact of Interventions on an Epidemic of Ebola in Sierra Leone and Liberia. *PLOS Current Outbreaks* doi:10.1371/currents.outbreaks.4d41fe5d6c05e9df30ddce33c66d084c (2014).

[52] Valdez, L. D., Rêgo, H. H. A., Stanley, H. E., & Braunstein, L. A. Predicting the extinction of Ebola spreading in Liberia due to mitigation strategies. arXiv preprint arXiv:1502.01326 (2015)

Author Contribution Statement

L.G.A.Z. and L.A.B. wrote the main manuscript text and L.G.A.Z. prepared figures 1-4. All authors performed the research and reviewed the manuscript.

Supplementary Information

To measure the efficiency of the our SI_IR model we focus on a two-layer network in which one layer is isolated. The two layers of our network, A and B, are of equal size N. This situacion reflects a real-world scenario in which infected individuals do not go to their jobs, layer A, but still have contact with people, layer B. At the initial stage all the individuals in both layers are susceptible. We randomly infect a node in layer A. This node can either be isolated within its own layer with a probability w for a period of time t_w or spread the disease within its own layer with a probability $1-w$. Also, it will be present in layer B and will spread the disease there. Thus the isolated nodes in network A will be able to infect for a shorter period of time than the non-isolated nodes, and the transmissibility of isolated individuals will be $1-(1-\beta)^{t_r-t_w}$. On the other hand, the transmissibility of non-isolated individuals in A and all infected individuals in B will be equal to $1-(1-\beta)^{t_r}$. At the final stage of the propagation all individuals are either susceptible or recovered, and the transmissibility T^A and T^B for each layer is given by

$$\begin{aligned} T^A &= 1-\left[(1-w)\,(1-\beta)^{t_r}+w\,(1-\beta)^{t_r-t_w}\right], \\ T^B &= 1-\left[(1-\beta)^{t_r}\right]. \end{aligned} \tag{5}$$

Here the second and third term of T^A takes into account non-isolated and isolated individuals in layer A and represents the probability that an infected individual will not transmit the disease during the t_r and t_r-t_w time steps, respectively. In layer B the transmissibility is the same as in the SIR model.

Using the theoretical arguments presented in Model and Simulation Results we can write two self-consistent coupled equations, f_i, $i=A,B$,

$$\begin{aligned} f_A &= [1-G_1^A\,(1-T^Af_A)\,G_0^B(1-T^Bf_B)] \\ f_B &= [1-G_1^B(1-T^Bf_B)\,G_0^A(1-T^Af_A)], \end{aligned} \tag{6}$$

from which we can obtain the critical threshold β_c (see Model and Simulation Results) in which

$$(T_c^AT_c^B)^2\,[(\kappa_A-1)(\kappa_B-1)-\langle k_A\rangle\langle k_B\rangle]-T_c^A(\kappa_A-1)-T_c^B(\kappa_B-1)+1 \;=\; 0. \tag{7}$$

Here κ_A and κ_B are the branching factor of layers A and B, and $\langle k_A\rangle$ and $\langle k_B\rangle$ are their average degree. Figure 5 shows a plot of the phase diagram in the plane $\beta-w$ for (a)

two ER multilayer networks [41] with average degree $\langle k_A \rangle = \langle k_B \rangle = 2$ and (b) two power law networks with an exponential cutoff $c = 20$ [7], with $\lambda_A = 2.5$ and $\lambda_B = 3.5$. In Fig. 5 we use $t_r = 6$ and values $t_w = 0, 1, 2, 3, 4, 5$, and 6, reading from bottom to top.

Note that the regions below the curves in Fig. 5 correspond to the epidemic-free phase. Then for different values of t_w these regions widen as w increases and reach their maximum size for t_r equal to t_w. Unlike the model with isolation in both layers (see Fig. 3 in Model and Simulation Results), as t_w increases the critical values of β change as w increases. When $t_w = 0$ and $w = 0$ we recover the SIR process in a two-layer network that corresponds to $\beta_c \approx 0.043$ with $k_{\min} = 1$ and $k_{\max} = 40$ in Fig. 5(a) and $\beta_c \approx 0.019$ with $k_{\min} = 2$ and $k_{\max} = 250$ in Fig. 5(b). In contrast to the model with isolation in both layers there is no critical value of w above which there is only an epidemic-free phase. Thus we conclude that this model is not as efficient in halting the spreading as the model with isolation in both layers.

Note that an isolation may represent a behavioral change, but unlike previous models in which the behavioral changes are solely the result of decisions made by susceptible individuals, our model also allows behavioral changes brought about by placing the individuals in quantantine or by hospitalizing them [48, 50–52], two practices that were instituted during the recent Ebola outbreak in West Africa.

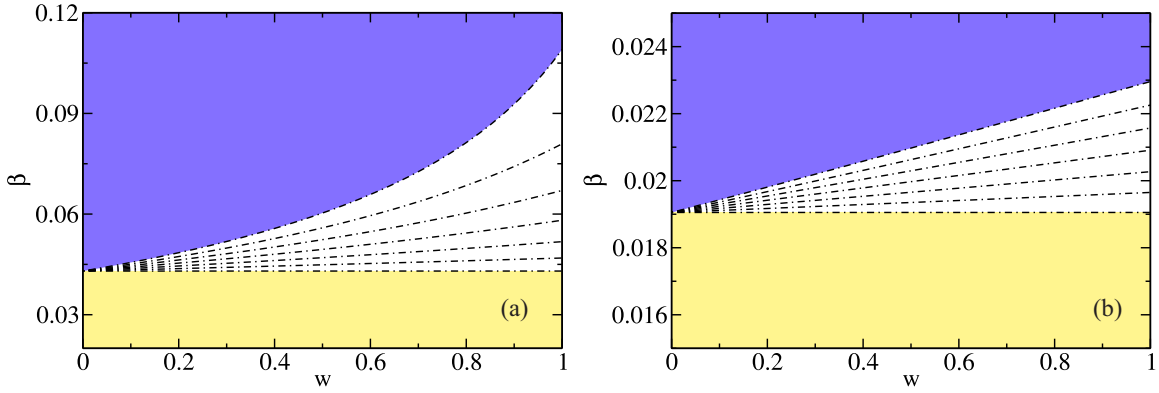

FIG. 5: Phase diagram in the plane $\beta - w$. In both plots, we consider $t_r = 6$ and $t_w = 0, 1, 2, 3, 4, 5, 6$ from bottom to top for (a) two ER networks with $\langle k_A \rangle = \langle k_B \rangle = 2$ with $k_{\min} = 1$ and $k_{\max} = 40$. (b) two power law networks with $\lambda_A = 2.5$ and $\lambda_B = 3.5$ with $k_{\min} = 2$ and $k_{\max} = 250$ and exponential cutoff $c = 20$. The region above each line corresponds to the Epidemic phase and the region below correspond to the Epidemic-free phase. In the limit of $w \to 0$ and for $t_w = 0$ we recover the SIR in multiplex networks with (a) $\beta_c \approx 0.043$ and (b) $\beta_c \approx 0.019$.